Mon. Not. R. Astron. Soc. **000**, 000–000 (0000) Printed 1 February 2008 (MN LATEX style file v1.4)

Evidence against field decay proportional to accreted mass in neutron stars

Ralph A.M.J. Wijers
Institute of Astronomy, Madingley Road, Cambridge CB3 0HA, UK
Email: R.Wijers@ast.cam.ac.uk

submitted to MNRAS, 24-7-96, revised 27-11-96, accepted 02-01-97

ABSTRACT
A specific class of pulsar recycling model, in which magnetic-field decrease is a function only of the amount of mass accreted onto the neutron star, is examined in detail. It is shown that no model in this class is consistent with all available data on X-ray binaries and recycled pulsars. Only if all constraints are stretched to their limit and a few objects (PSR B1831−00 and 4U 1626−67) are assumed to have formed in a non-standard manner is there still an acceptable model of this kind left. Improved measurements of the parameters of a few of the oldest known radio pulsars will soon test and probably rule out that one as well. Evidence for the origin of PSR B1831−00 via accretion-induced collapse of a white dwarf is called into question as a result.

Key words: pulsars: recycled – neutron stars: structure – neutron stars: magnetic fields – X-ray binaries

1 INTRODUCTION

The growing body of evidence against rapid spontaneous magnetic-field decay in neutron stars (Kulkarni 1986; Verbunt, Wijers, & Burm 1990; Bhattacharya et al. 1992) has led to the hypothesis that pulsar magnetic fields are lowered by recycling in binaries (see Bhattacharya & Van den Heuvel 1991 for a review). The mechanism for this remains unclear, with suggestions including decay of crustal fields due to heating (Blondin & Freese 1986) or burial of the field (Bisnovatyi-Kogan & Komberg 1975; Romani 1990, 1993) and decay of core fields due to flux tube expulsion from the superfluid interior (Srinivasan et al. 1990).

A heuristic model first suggested by Taam and Van den Heuvel (1986) and explored further by Shibazaki et al. (1989) is that the ratio of initial to final magnetic field is simply proportional to the amount of mass accreted. The detailed model by Romani (1993) supports this in the regime of high accretion rates. Van den Heuvel and Bitzaraki (1995) have shown that it is consistent with the magnetic fields of most recycled pulsars with helium white dwarf companions. In this paper the model (and a generalised version of it) is tested for agreement with a wider body of data including many types of neutron star binary, and it fails the test.

The details of the model used to evolve pulsar periods and fields is discussed in Section 2. The constraints derived from applying the model to observed neutron stars are presented in Section 3; some further discussion of the implications (Section 4) and an outline of the main conclusions (Section 5) follow.

2 THE MODEL

2.1 Neutron star structure

The amount of mass accreted onto recycled pulsars can approach $\mathrm{M}_\odot$, so we should follow the concomitant change of radius and moment of inertia. To compute the gravitational mass, M_g, as a function of baryon mass, M_b, I use the binding energy correction given by Lattimer & Yahil (1989):

$$M_\mathrm{b} = M_\mathrm{g} + 0.084\mathrm{M}_\odot \left(\frac{M_\mathrm{g}}{\mathrm{M}_\odot}\right)^2 \quad (1)$$

As M_b increases by accretion, M_g increases more slowly. The mass dependence of the radius is taken to be

$$R_6 = \frac{R}{10\,\mathrm{km}} = \left(\frac{M_\mathrm{g}}{1.4\mathrm{M}_\odot}\right)^{-1/3} \quad (2)$$

and assuming the radius of gyration is a constant fraction of R the moment of inertia will be

$$I_{45} = \frac{I}{10^{45}\,\mathrm{g\,cm^2}} = \left(\frac{M_\mathrm{g}}{1.4\mathrm{M}_\odot}\right)^{+1/3}. \quad (3)$$

Here the normalisation is chosen to get the 'standard' values $I_{45} = 1$ and $R_6 = 1$ for a $1.4\mathrm{M}_\odot$ neutron star. Test calculations show that modest deviations from the above do not affect the conclusions. After accreting $1\mathrm{M}_\odot$ onto a $1.4\mathrm{M}_\odot$ neutron star we have $M_\mathrm{g} = 2.05\mathrm{M}_\odot$, which exceeds the maximum mass for a significant number of equations of state. To be conservative, I shall just assume that accretion does not lead to the collapse of the neutron star into a

black hole rather than use the maximum mass as an extra constraint.

2.2 Magnetic field evolution

Since both the magnetic fields and the amounts of accreted mass of neutron stars vary by many powers of ten, any model relating the two will almost necessarily be a power law:

$$\frac{B}{B_0} = \left(1 + \frac{\Delta M}{M_\mathrm{c}}\right)^{-\beta}. \quad (4)$$

B and B_0 are the current and initial field, ΔM is the accreted (baryon) mass, and M_c is the characteristic mass at which field decrease becomes significant. For $\beta = 1$ this is the well-known scaling relation proposed by Taam & Van den Heuvel (1986) and Shibazaki et al. (1989). I have added the exponent because the generalisation probably encompasses effectively all models in which B depends on ΔM only. Once the amount of accreted mass becomes enough to affect the radius of the neutron star, one should perhaps consider changes in the surface field due to conservation of magnetic flux BR^2, but here I use Eq. 4 throughout.

2.3 Spin evolution

Another constraint on the decay model is imposed by the fact that some recycled pulsars are spinning very rapidly, near their equilibrium period. For low fields and/or low accretion rates the accreted mass cannot carry the required angular momentum to the neutron star. To follow the evolution in this phase I use the torque model for disc accretion by Ghosh & Lamb (1979). The spin-up rate is given by

$$\dot{P} = -3.6{\times}10^{-4} B_{12}^{2/7} R_6^{6/7} I_{45}^{-1} M_{1.4}^{3/7} \dot{M}_{-8}^{6/7} P^2 n(\omega_\mathrm{s}) \quad \mathrm{s\,yr^{-1}}, \quad (5)$$

where $B_{12} = B/10^{12}\,\mathrm{G}$ and $\dot{M}_{-8} = \dot{M}/10^{-8}\,\mathrm{M_\odot\,yr^{-1}}$. ω_s (called fastness) is the ratio of neutron star spin frequency to the Kepler frequency of an orbit just outside the magnetopause and $n(\omega_\mathrm{s})$ is the dimensionless torque function which is given approximately by

$$n(\omega_\mathrm{s}) = 1.39 \frac{1 - \omega_\mathrm{s}[4.03(1-\omega_\mathrm{s})^{0.173} - 0.878]}{1 - \omega_\mathrm{s}}. \quad (6)$$

The fastness is related to the spin period by

$$\omega_\mathrm{s} = 0.43 B_{12}^{6/7} R_6^{18/7} M_{1.4}^{-5/7} \dot{M}_{-8}^{-3/7} P^{-1}. \quad (7)$$

($M_{1.4} = M_\mathrm{g}/1.4\mathrm{M_\odot}$) Since the physics of the interaction between accretion disc and magnetosphere is uncertain and the expressions also depend on the poorly understood structure of the accretion disc itself, there is ample uncertainty in the torque. For the present purpose it is adequate, however. The value of the critical fastness, ω_cr, at which the torque vanishes (0.349 for Eq. 6) is important, so the effect of changing it is examined below. Setting $\omega_\mathrm{s} = \omega_\mathrm{cr}$ in Eq. 7 fixes a relation $P_\mathrm{eq} \propto B^{6/7}$ called the spinup line or equilibrium spin period.

2.4 Initial conditions

In the calculations all neutron stars start with a gravitational mass, M_g, of $1.4\mathrm{M_\odot}$ (so $M_\mathrm{b} = 1.56\mathrm{M_\odot}$). The accretion rate is taken to be constant, with a usual value of $2{\times}10^{-8}\,\mathrm{M_\odot\,yr^{-1}}$, the Eddington rate for electron scattering opacity on material with hydrogen mass fraction $X = 0.7$ onto a 10 km neutron star. Pulsars with initially high fields retain no memory of their initial spin periods once they reach fields below about 10^{10} G when they are evolved using the above equations. Since the only pulsars to which spin constraints are applied here have lower fields than this, the initial period does not matter, and all pulsars are started at $P = P_\mathrm{eq}$. For very short-lived accretion phases that start when the pulsar is still spinning very rapidly (e.g. Brown 1995) this is not correct, because the pulsar will then eject mass thrown towards it and never accrete. This more complicated situation is treated elsewhere (Wijers, Braun, & Brown 1997).

The initial magnetic field is that of young radio pulsars, which at birth have $\log B_0 = 12.3$ typically, with a spread around that of a factor 2. To investigate the influence of the initial field I compute all results for $\log B_0 = 11.8$, 12.3, and 12.8. This range nominally covers 87% of all pulsars in the best-fit initial magnetic field distribution found by Hartman et al. (1996). In assembling the final constraints on the parameters M_c and β I use whichever value in this range is least constraining to the accretion-induced decay model. Therefore all the derived bounds are necessarily somewhat statistical in nature rather than absolute, because some 7% of pulsars will lie outside an indicated range on either side.

2.5 Example evolution tracks

Fig. 1 shows the lower left corner of the radio pulsar period-magnetic field diagram with the known pulsars from the Princeton catalogue (Taylor, Manchester, & Lyne 1993, as updated by Taylor et al. 1995) indicated as open symbols. The filled symbols with names are the pulsars that are discussed below. Their properties are listed in the top part of Table 1. For pulsars close to the Hubble line (lower dotted curve) the value of the magnetic field derived from the period derivative (B_m in Table 1 and filled squares in Fig. 1) should be corrected for the proper motion of the pulsar which contributes to the measured period derivative (Shklovskii 1970; Camilo, Thorsett, & Kulkarni 1994). The corrected values (B_e in Table 1 and filled triangles in Fig. 1) are estimates based on an assumed $75\,\mathrm{km\,s^{-1}}$ transverse velocity, except for PSR J2317+1439, where a transverse velocity of $70\,\mathrm{km\,s^{-1}}$ has been measured (Camilo, Nice, & Taylor 1996a).

All evolution tracks shown in Fig. 1 are for $\log B_0 = 12.3$ and $\dot{M}_{-8} = 2$. The dashed-dotted curves are for $\beta = 1$ and $\mu_\mathrm{c} \equiv \log(M_\mathrm{c}/\mathrm{M_\odot}) = -5$ (lower) and $\mu_\mathrm{c} = -3$ (upper). The curve for low μ_c passes nicely through the millisecond pulsar range but misses the fastest ones. For high μ_c the lowest fields are not reached (the tracks in Fig. 1 all end at $\Delta M = 0.8\mathrm{M_\odot}$). The intermediate case $\mu_\mathrm{c} = -4$ (not shown) almost follows the standard spinup line (heavy solid curve) and is acceptable. The curve for $\mu_\mathrm{c} = -3$ illustrates the importance of the changing neutron star mass: PSR B1821−24 appears to be above the spinup line, but that is drawn for a fixed neutron star mass of $1.4\mathrm{M_\odot}$, as is traditional. Increasing the mass shifts the spinup line to the left enough to reach this pulsar without exceeding $\dot{M}_{-8} = 2$.

Low fields can be reached with $\mu_\mathrm{c} = -3$ by increasing β. This is illustrated by the dashed ($\beta = 1.5$) and solid

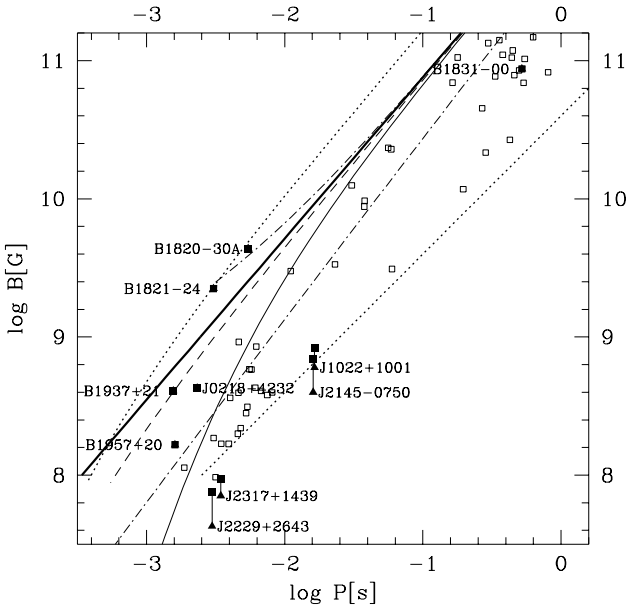

Figure 1. The lower left corner of the B-P diagram of radio pulsars. Open squares denote pulsars, filled symbols with names are those specifically discussed in this paper. The lower dotted line indicates a characteristic age, $P/2\dot{P}$, of 10 Gyr, the heavy solid line is the standard spinup line. The other curves are evolution tracks of pulsars, explained in the text.

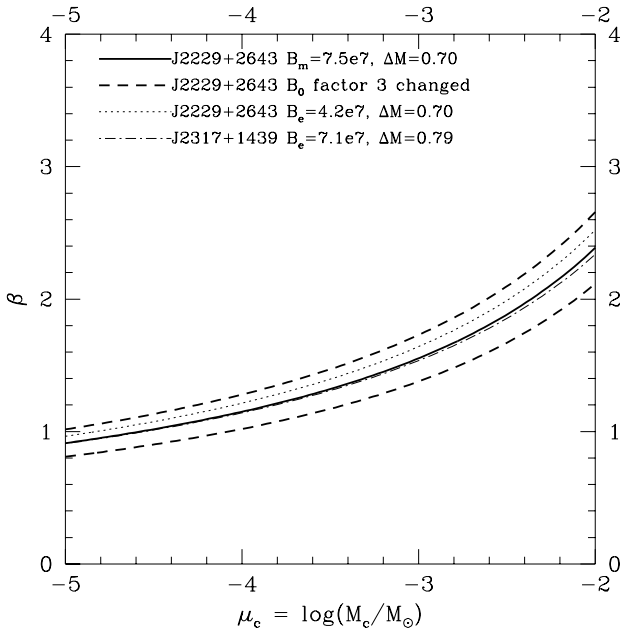

Figure 2. Constraints in the $(M_{\rm c}, \beta)$ plane imposed by the lowest-field pulsars

($\beta = 2$) curves. The dashed curve is fully acceptable for any of the fast, low-field pulsars, whereas the $\beta = 2$ case does not produce the fast ones because the field has decayed to low values before enough mass has been accreted to spin the pulsar up. To shift the evolution track further to the left so that PSR B1821−24 can be reached, one can either increase the accretion rate or increase the value of the critical fastness. The latter option is illustrated by the dotted curve, for which $\omega_{\rm cr} = 0.7$, twice the standard value (see Section 3.2).

Once accretion stops, pulsars will start spinning down, so many pulsars that lie to the right of any track can be explained by evolution along that track down to some field strength and subsequent spindown. For pulsars with ages greater than the age of the universe (i.e. below the Hubble line) this will not work, so they must have emerged from the accretion phase with long periods, close to the current values. This poses no problems because for any evolution track that passes to the left of a given pulsar there is one with a lower accretion rate and otherwise the same parameters that passes through it. Such a low accretion rate may impose constraints on binary evolution scenarios, but I shall not attempt to exploit this here, and use only the requirement that the fastest pulsars be produced (Section 3.2).

3 CONSTRAINTS ON β AND $M_{\rm C}$

3.1 The weakest fields: PSR J2229+2643 and J2317+1439

The two lowest-field pulsars known are PSR J2229+2643 and J2317+1439 (Camilo et al. 1996a). Both are in binaries with low-mass white dwarf companions for which Van den Heuvel and Bitzaraki (1995) estimated the amount of mass accreted by the pulsar to be $0.70{\rm M}_\odot$ and $0.79{\rm M}_\odot$, respectively. Some properties are listed in Table 1.

For PSR J2229+2643, I use the measured field $B_{\rm m}$ because the proper motion has not been measured and therefore its $B_{\rm e}$ is only based on a typical value (see above). For PSR J2317+1439 the proper motion is measured, so I use $B_{\rm e}$. The solid line in Fig. 2 is the locus of parameter values that yields the field of PSR J2229+2643 for its ΔM, and the dashed-dotted curve the same for PSR J2317+1439, both for $\log B_0 = 12.3$. They are almost the same, since the slightly lower field of PSR J2317+1439 and its higher ΔM act in opposite directions. Using $B_{\rm e}$ for PSR J2229+2643 gives the dotted curve. The higher curve here gives the strongest overall constraint, so I use the solid curve in our final assembly of constraints, but I still have to account for the variation in B_0. The dashed curves are as the solid one, but for $\log B_0 = 12.8$ (upper) and 11.8 (lower). They also roughly bracket the range 0.4–$1.5{\rm M}_\odot$ for ΔM at fixed $\log B_0 = 12.3$. Given the uncertainty in B_0, the entire region between the two dashed curves satisfies the requirement that low enough fields be attainable.

3.2 The fastest pulsars: PSR B1937+21 and B1821−24

As explained above (Section 2.5), the only spin constraint applied is that fast enough pulsars can be formed. For $\dot{M}_{-8} = 2$ and $\omega_{\rm cr} = 0.35$ the strongest constraint on the model is set by PSR B1937+21, the lowest-field pulsar close to the spinup line. The thick solid line in Fig. 3 indicates the locus of models that pass exactly through its current position in the period-field diagram, for $\log B_0 = 12.3$. All models below the curve are allowed, those above it are excluded. The thick dashed lines indicate how the curve changes for $\log B_0 = 12.8$ (upper) and 11.8 (lower). The next strongest constraints for the same accretion rate are

Table 1. Relevant properties of the systems used. Radio pulsars are at the top, X-ray pulsars at the bottom. $B_{\rm m}$ is the field measured from the radio pulsar spindown rate, $B_{\rm e}$ is the field after correcting for proper motion; for X-ray pulsars it is the field for which the pulsar would be on the spinup line. Pulsar companion masses are taken from Van den Heuvel & Bitzaraki (1995). X-ray binary parameters are taken from Van Kerkwijk, Van Paradijs & Zuiderwijk (1995). $\dot{M}_{-8}$ is estimated from the X-ray luminosity.

name	$P_{\rm spin}$ (s)	$P_{\rm orb}$ (d)	companion type	companion mass ($M_\odot$)	$\log B_{\rm m}$ (G)	$\log B_{\rm e}$ (G)	$\dot{M}_{-8}$	$\tau_{\rm X}$ (10^4 yr)	ΔM ($M_\odot$)
PSR J0218+4232	0.00232	2.03	He WD	0.20	8.63				
PSR J1022+1001	0.0165	7.8	CO WD	>0.45	8.92	8.8			0.01–0.045
PSR B1820−30A	0.00544		single		9.64				
PSR B1821−24	0.00305		single		9.35				
PSR B1831−00	0.521	1.81	He WD?	0.20?	10.94				0.80
PSR B1937+21	0.00155		single		8.61				
PSR B1957+20	0.00161	0.382	?	>0.02	8.22				
PSR J2145−0750	0.0161	6.84	CO WD	>0.45	8.84	8.6			0.01–0.045
PSR J2229+2643	0.00298	93.0	He WD	0.30	7.88	7.6			0.70
PSR J2317+1439	0.00345	2.46	He WD	0.21	7.97	7.8			0.79
SMC X-1	0.717	3.89	B0Ib	15.		12.0	4	2	8×10^{-4}
LMC X-4	13.51	1.41	O7III–V	16.		13.6	5	1	5×10^{-4}
Cen X-3	4.84	2.09	O6.5II–III	19.		12.7	1	1	1×10^{-4}
Her X-1	1.24	1.7	A–FIV	2.3		11.7	0.2	30	6×10^{-4}

provided by PSR B1957+20 and J0218+4232. Their curves for $\log B_0 = 12.3$ nearly coincide with the upper dashed line and have not been plotted separately. For no curve shown is the required amount of accreted mass greater than $0.8M_\odot$, and for the thick solid line it is about $0.3M_\odot$ everywhere on it. The constraint is tighter for a lower accretion rate because it puts PSR B1937+21 closer to the equilibrium period. The thin solid curve differs from the thick one only in that $\dot{M}_{-8} = 1$, but the difference is small. The dotted curve illustrates what happens if the change of mass of the neutron star is neglected, but all parameters are as for the thick solid curve: it leads to an artificially stronger constraint because it does not allow the spinup line to move to shorter periods as the neutron star mass increases (see Fig. 1).

Next we must consider what to do with PSR B1821−24 and B1820−30A, which are above the standard spinup line. Both these pulsars are in globular clusters and it is possible that their location is a consequence of a type of evolution that is unique to that environment (e.g. a dramatic period of mass transfer following a collision with another star), so perhaps we should omit them from the discussion. The location of PSR B1820−30A could even be a direct result of contamination of its period derivative due to acceleration in the cluster potential (Biggs et al. 1994). But since I use standard spinup theory, it is appropriate to at least briefly ask whether their location above the standard spinup line indicates a flaw in that theory that is serious enough to reconsider its use.

Increasing the mass of the neutron star helps to bring it above the standard spinup line, but it turns out that models in which these still relatively high-field neutron stars have become heavy enough cannot produce the lowest observed fields. One possible remedy is to accept higher accretion rates, as observed in some X-ray pulsars (see Sect. 3.3). If we set $\dot{M}_{-8} = 6.2$ both pulsars are on the spinup line. It turns out that the strongest constraint on models is then set by PSR B1821−24, and nearly coincides with the lower dashed line, so it would provide a stronger constraint. Another option is to increase the critical fastness to 0.7 by using a toy model $n(\omega_{\rm s}) = 1.39(1-\omega_{\rm s}/0.7)/(1-\omega_{\rm s})$. Once again PSR B1821−24 provides the strongest constraint, shown by the thin dashed curve ($\log B_0 = 12.3$); varying the initial field produces similar offsets to the case of PSR B1937+21. In other words, simple and reasonable adjustments to standard spinup theory can accommodate these two pulsars, and would give stronger constraints. Due to the location of the pulsars in globular clusters and the consequent possibility that they evolved in a manner radically different from disc pulsars, it is better not to use those constraints.

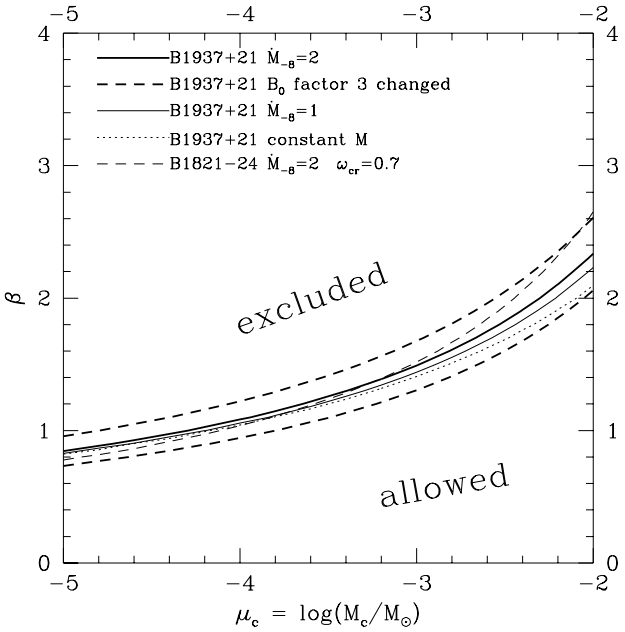

Figure 3. Constraints in the $(M_{\rm c}, \beta)$ plane imposed by the fastest pulsars.

The weakest constraint from pulsar fastness is the up-

per dashed curve or the thin dashed curve displaced upwards as appropriate for $\log B_0 = 12.8$. Which one is used matters little once it is combined with the constraint set in the previous section. The area that satisfies the most conservative constraints from Figs. 2 and 3 is shown in Fig. 4 as the hatched region. It is mostly determined by the field of PSR J2229+2643, with a minor contribution from the spin of PSR B1937+21 at low $\log M_c$.

3.3 X-ray pulsars

The classical high-mass X-ray binaries contain high-field neutron stars. To estimate their amounts of accreted mass we need the accretion rate, which can be derived from the observed X-ray luminosity, and the X-ray life time, for which models are required. The finally adopted values for the four X-ray binaries SMC X-1, LMC X-4, Cen X-3, and Her X-1 are listed in Table 1.

The X-ray luminosities were taken from White, Swank, & Holt (1983) and are somewhat higher than often quoted. This is because X-ray pulsars have hard spectra and usual fluxes are cited in the range 2–10 keV. But White et al. quote luminosities from 0.5–60 keV, which much better represent the total luminosity, as can be seen from the spectra they show. All four sources are disc accretors and are not expected to vary too much in flux. For example, a low flux is sometimes seen for SMC X-1 (e.g. Seward & Mitchell 1981), but a 7-year monitoring using the Vela 5B satellite (Whitlock & Lockner 1994) shows an average 3–12 keV luminosity of 2×10^{38} erg s^{-1} despite the occasional low state, quite consistent with the 2.5 times higher value for the wider energy range quoted by White et al. The X-ray luminosities were converted to accretion rates assuming that $L_X = GM\dot{M}/R$, with $M = 1.4\mathrm{M}_\odot$ and $R = 10$ km.

One might worry that beaming of the X-ray pulsar radiation causes an overestimate the luminosity because we are hit by the beam but other positions in the sky are not, and our estimates assume isotropic emission. For radio pulsars, which have very narrow beams, this clearly a concern. But X-ray pulsar profiles are very different: inspection of the pulse profiles in White et al. (1983) reveals that significant emission is present over the full 360° of pulse phase, and the rms. variation of the intensity over phase is 0% for Cen X-4, 5–20% for SMC X-1, 20–50% for Her X-1 and 50% for Cen X-3. (Ranges are given if the modulation depth depends on energy band.) Since these are very bright sources, they would be detected even if the phase-average flux were as low as the lowest flux that occurs at any phase. This is unlike radio pulsars, many of which go undetected because their beam is never pointed towards us. Since the flux variation in the direction perpendicular to the beam sweep is unlikely to be very different from the one along the pulse, X-ray pulsars are detectable from any direction in the sky. This means that (i) the phase-averaged flux we see is unlikely to deviate much from the mean over the entire sphere around the pulsar and (ii) the deviation could be positive or negative, i.e. in a sample of pulsars we will not systematically overestimate the luminosity. Therefore, the estimated amounts of transferred mass are not systematically biased upwards due to beaming.

To estimate the X-ray life times I use the model of beginning atmospheric Roche lobe overflow (Savonije 1978, 1979). In this model, the donor star is still burning hydrogen in its core, but extended in size due to mass loss. It expands on a nuclear time scale and the mass transfer rate grows exponentially with an e-folding time, τ_X, equal to the time it takes the star to expand by one scale height. For massive donors this time scale is about 10^4 yr, in agreement with the estimated X-ray life time from population statistics (Meurs & Van den Heuvel 1989). Her X-1 has a subgiant donor of much lower mass, so its life time is rather longer. The values shown in Table 1 are taken from Savonije. Since the accretion rate grows exponentially, ΔM is well approximated by τ_X times the current accretion rate.

The magnetic fields of X-ray pulsars are high, but precise values are hard to specify. The estimate in Table 1 is based on the assumption that the pulsar is on the equilibrium spinup line, but only for Her X-1 is the spinup time scale sufficiently shorter than τ_X to justify this assumption. The cyclotron line feature seen in the spectrum of Her X-1 indicates a surface field of 3×10^{12} G (Trümper et al. 1978), in good agreement with the spinup estimate given that the cyclotron line probes the field very near the neutron star, whereas the spinup estimate probes the large-scale dipole field. No cyclotron lines have been seen from the other three X-ray pulsars. Since they had lower accretion rates and therefore longer equilibrium periods in the past and are spinning up, their equilibrium periods are probably shorter and therefore the field strengths are overestimates.

If we assume that the four pulsars have had a factor 3 field decrease each one defines a curve in the (M_c, β) plane that is shown in Fig. 4. (A small systematic difference between their fields and those of standard radio pulsars cannot be ruled out, but a factor 10 is too much. A factor 3 is a reasonable estimate of what might still be allowed.) The area below and to the right of the curves corresponds to lower amounts of field decrease and is thus allowed. The area above them is excluded. The three curves defined by LMC X-4, Her X-1, and SMC X-1 are quite similar. I shall take the middle one (Her X-1) to fairly represent the X-ray pulsar constraint. The allowed region thus left no longer contains any combination with $\beta = 1$, so the standard model in which field decay is proportional to accreted mass is already ruled out.

3.4 PSR J2145−0750

A recently discovered class of millisecond pulsars with high-mass CO white dwarf companions provides us with a probe of the regime of ΔM in between the X-ray pulsars and the most strongly recycled pulsars. Van den Heuvel (1994) discusses their evolution in detail and concludes that the progenitor of the white dwarf was a 1–6$\mathrm{M}_\odot$ star that came into Roche contact on the asymptotic giant branch. The amount of accreted mass is mainly from wind accretion and increases from 0.01 to 0.045$\mathrm{M}_\odot$ with increasing donor mass. For the highest, least constraining amount of accreted mass, and for $\log B_m = 8.84$ for PSR J2145−0750 (based on $\dot{P} = 2.98\times10^{-20}$, F. Camilo, private communication) the curve of acceptable parameter pairs is shown in Fig. 4 for $\log B_0 = 12.3$ (solid), 12.8 (upper dotted), and 11.8 (lower dotted). The lower curve just grazes the still acceptable region at $(-3.2, 1.6)$, so if one wants to keep a field decay model from this class these are its parameters. More likely,

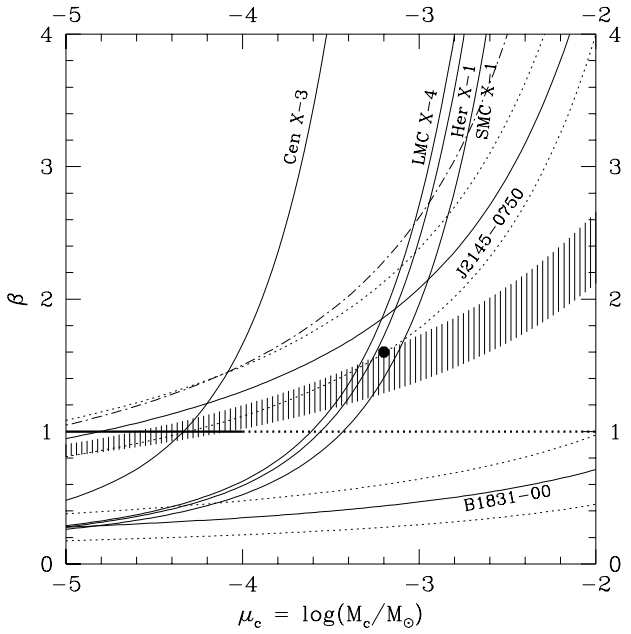

Figure 4. Summary of all constraints in the (M_c, β) plane. The black dot marks the location of the model that is still marginally consistent with all constraints except PSR B1831−00.

one cannot in reason stretch all the constraints to their limits simultaneously and the model is inconsistent with the whole body of available data. The best prospect for ruling it out altogether comes from PSR J2145−0750 and its twin sister, PSR J1022+1001 (Camilo et al. 1996a). Both have significant estimated proper-motion corrections to the magnetic field (see Fig. 1 and Table 1), so the lower values of the corrected fields will push the curve up and remove it further from the area allowed by the constraints. Also, not all will have had the maximum allowed accreted mass. To indicate the strong effect of this I show the acceptable curve for PSR J2145−0750 for the same parameters as the solid curve except that $\Delta M = 0.02\mathrm{M}_\odot$ (dashed-dotted). It leaves no acceptable parameter combinations.

4 DISCUSSION

4.1 PSR B1831−00 and 4U 1626−67: Accretion-induced collapse?

In the previous section I have deliberately not included two objects that have been adduced as good evidence against field decay proportional to accreted mass in the past: PSR B1831−00 and the X-ray pulsar 4U 1626−67. The ages and orbital parameters of both suggest that the neutron star has accreted at least $0.5\mathrm{M}_\odot$, yet the fields are high (Verbunt et al. 1990). The reason is that at various times accretion-induced collapse (AIC) of a white dwarf has been proposed as a method of making these, allowing the neutron star to have accreted less mass than it seems, so I wanted to make the case against the decay model without them. Also, both have peculiarly low companion masses so they may really be different.

But let us briefly revisit PSR B1831−00. It has $B = 8.7 \times 10^{10}$ G and $P_{\rm orb} = 1.8$ d. Van den Heuvel and Bitzaraki (1995) claim that its position at high field is good evidence for accretion-induced collapse of a white dwarf. In this scenario, the accreting object in the binary was a white dwarf while most of the donor mass was accreted, but near the end of accretion it reached the Chandrasekhar mass and collapsed to a neutron star, which then accreted little enough to keep a high field. For the standard $\beta = 1$ model they used this may still be reasonable, since the accreted amount after collapse could be $0.1\mathrm{M}_\odot$. This is a fair fraction of the total transferred ($\sim 0.8\mathrm{M}_\odot$) so the moment of collapse need not be tuned too delicately. But the most tolerable model still left now ($\beta = 1.6, \mu_c = -3.2$) limits the amount of accreted mass to $0.01\mathrm{M}_\odot$, even if we allow the pulsar to start with a 10^{13} G field. This does require the collapse to be rather finely timed very near the end of accretion, and makes the scenario quite unattractive. Even if one were willing to accept this fine tuning for PSR B1831−00, there is still the following coincidence: why should it be the only short-period binary pulsar with such a high field? After all, there must have been less fortunately timed cases like it, in which the collapse occurred less close to the end of mass transfer. The resulting neutron stars would have lower fields, between that of PSR B1831−00 and the canonical low values, and therefore live longer and be more abundant. Note that this problem occurs no matter which parameters one chooses for the decay model. Consequently, I feel that one should accept the fact that it has accreted significant amounts of mass, as has 4U 1626−67. This is of course fatal to the decay model, as illustrated by the lowest curves in Fig. 4, which define the region of acceptable parameters to fit PSR B1831−00 (using $\Delta M = 0.8\mathrm{M}_\odot$ and $\log B_0 = 11.8, 12.3, 12.8$).

AIC has at various times in the past been called on to rescue the then popular field decay model, by providing an alternative formation mechanism for the few objects that obviously failed to fit the model. So it was when Her X-1 failed to fit the rapid exponential decay of neutron star magnetic fields, but Verbunt et al. (1990) showed that AIC cannot provide a viable alternative in that case and that therefore Her X-1 does disprove the model. It will remain a matter of taste in each case whether to view the lone strange object as an exception that proves the model or a nail its coffin. But in the case of PSR B1831−00 and 4U 1626−67 the exceptions are once again nails, if not the only ones, and AIC cannot change this (This argument was already partly given by Verbunt et al. 1990.)

4.2 Constraints on field only

Since the spin period constraints did not contribute too much to constraining the field decay model, it is possible to capture most of the argument in a straight plot of amount of field change versus accreted mass (Fig. 5). Each diamond represents one object whose name is plotted alongside it. The size of the diamond represents the error in the location of the object. Most of the 'errors' in the quantities ultimately include uncertainties in the models used to interpret the data from which the quantities are derived and they therefore are indicative of the author's personal assessment of those models rather than well-defined statistical quantities. The error in the ratio B/B_0 was taken to be 0.5 dex and mainly represents the variation of initial magnetic fields of neutron stars; this range nominally covers 87% of initial

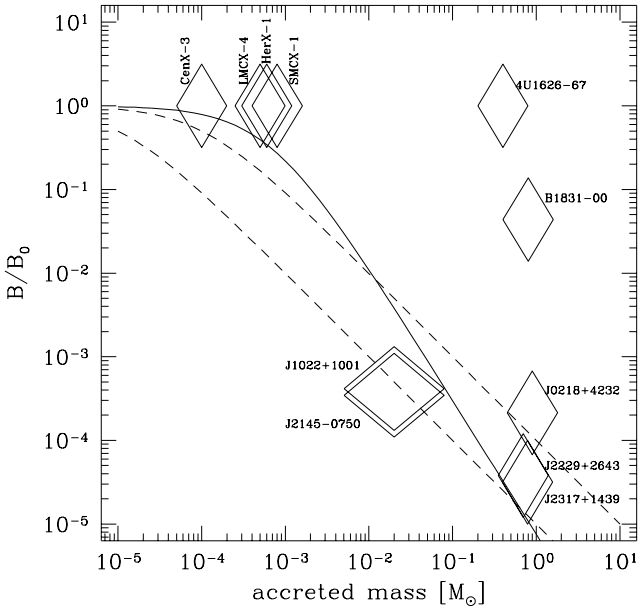

Figure 5. The accreted mass versus magnetic field for all objects in Table 1 except those that constrain the model through their spin period. The dashed curves are decay models with $\beta = 1$ and $\mu_c = -4$ (top) and -5 (bottom). The solid curve is for the model marked with a black dot in Fig. 4 ($\beta = -1.6, \mu_c = -3.2$).

fields (Sect. 2.4). The amounts of accreted mass for the X-ray pulsars are derived partly from theory and partly from data. Those of the millisecond pulsars are related via theory to system parameters that are accurately known observationally, so the error is mostly uncertainty in the theory. In all cases, I have assigned an error of a factor 2 either way to the estimated ΔM, which should be fairly generous. For PSR J1022+1001 and J2145−0750, the theoretical estimate itself already spans a factor 2 each way from the mean of $0.02\mathrm{M}_\odot$ (Table 1), so I have used a total error of a factor 4 either way for their ΔM. Given the generous errors used one should really demand that any model curve pass through 80% of all the diamonds. For any diamond that is widely missed, one will have to find an alternative model that puts the object in a completely different position.

The first striking impression from Fig. 5 is that the full range of accreted masses is represented by objects with little or no field decay, and the full range of amounts of field decay is represented by objects that have accreted around $0.5\mathrm{M}_\odot$. This bodes ill for any model that demands a strict relation between the two quantities. A few models are indicated as well: the dashed curves represent the standard version of the model, $\beta = 1$. They lie either too low for the X-ray pulsars or too high for PSR J1022+1001 and J2145−0750. The solid curve represents the marginal model indicated by the black dot in Fig. 4. It just grazes the corners of many error boxes, and is already in trouble at the right of the diagram, since its predicted fields there are almost too low for the lowest-field pulsars known, but many pulsars exist at that same amount of accreted mass and ten times higher fields (like PSR J0218+4232).

The really difficult objects for the accretion-decay model are 4U 1626−67 and PSR B1831−00. They cannot possibly satisfy any model of this type. The difficulties of advancing accretion-induced collapse for the formation of PSR B1831−00 (sect. 4.1) are even greater for 4U 1626−67, where the amount of accreted mass needs to be reduced by 3 orders of magnitude from the total amount of mass transfer that has occurred in the system before it comes close to fitting any of the models. But mass transfer in this system is still ongoing and very long-lived, so this neutron star would have to have formed almost literally yesterday by AIC to save the accretion-decay model.

It is tempting to conclude from Fig. 5 that a significant amount of accreted mass, while it does not guarantee much field decay, is at least a necessary condition for it, because there appear to be no objects in the lower left corner. But that conclusion is not valid because this absence may well be due to poor chances of detecting such sources. Imagine a neutron star with very little accreted mass that has had much field decay. If it were not accreting it could only be visible as a radio pulsar. But for it to be above the death line it would have to have been spun up, which is not possible without significant mass accretion. If it were an accreting source, chances of detection are small again because the small amount of accreted mass implies that either the accretion phase has to be very short or the accretion rate has to be very low.

4.3 Further implications for models

The detailed model by Romani (1993) does predict field decay proportional to accreted mass down to a bottom value of around 10^8 G with $M_c = 10^{-5} - 10^{-4}\mathrm{M}_\odot$, as long as the accretion rate is high. Since all the objects used in the present paper have accreted most of their mass at rates not far below the Eddington rate this model as it stands is excluded by the data.

The boundaries I have drawn are statistical in nature due to the possible variations in initial magnetic field (Sect. 2.4). But the range used everywhere covers almost 90% of initial fields, and for every type of constraint there are at least 2 objects which provide a nearly equally strong version of that constraint. Therefore it is highly unlikely that we have condemned the model unjustly because all pulsars used to constrain it are untypical of the average in a direction that is unlucky for the model.

It is of course possible to save the model by varying the parameters β and M_c between pulsars, but this would largely remove its attraction unless one had a prescription for what parameters to give to which kind of pulsar. Doing so would merely reinforce the main conclusion of the present paper, namely that other parameters than accreted mass alone influence significantly the decay of a neutron star's magnetic field.

5 CONCLUSION

I have explored the consequences of a popular neutron star magnetic-field decay model in which the decay is determined solely by the amount of accreted mass. The result is that no model of this type (Eq. 4) can satisfy all the known constraints derived from the fields, estimated amounts of accreted mass, and spin periods of a variety of recycled radio pulsars and X-ray binaries. Only if the constraints are all

stretched to their limit simultaneously and PSR B1831−00 and 4U 1626−67 are not required to fit is there a small parameter range for which it is still viable. The most used version of the model, in which field decay is proportional to the amount of accreted mass to the first power, is firmly ruled out even then.

An important constraint is provided by the pulsars with very high apparent ages near the Hubble line. Their observed period derivatives are affected by proper motion and should be revised downwards (Camilo et al. 1994). Once more of their proper motions have been measured the constraints on recycling models set by them will strengthen significantly. The other important constraint comes from the fact that some X-ray pulsars have high fields despite having accreted up to $10^{-3}\mathrm{M}_{\odot}$. Since this value is somewhat model dependent, a firmer quantitative understanding of the evolution of classical high-mass X-ray binaries would also help to constrain models of neutron star field decay.

ACKNOWLEDGEMENTS

I would like to thank F. Camilo for helpful comments during the preparation of this paper, the early communication of some of his results, and careful reading of an early version of the manuscript, and J. van Paradijs for his helpful suggestions.

REFERENCES

Bhattacharya, D. & van den Heuvel, E. P. J. 1991, Phys. Rep. 203, 1
Bhattacharya, D., Wijers, R. A. M. J., Hartman, J.-W., & Verbunt, F. 1992, A&A 254, 198
Biggs, J. D., Bailes, M., Lyne, A. G., Goss, W. M., & Fruchter, A. S. 1994, MNRAS 267, 125
Bisnovatyi-Kogan, G. S. & Komberg, B. V. 1975, Sov. Astron. 18, 217
Blondin, J. M. & Freese, K. 1986, Nature 323, 786
Brown, G. E. 1995, ApJ 440, 270
Camilo, F., Nice, D. J., Shrauner, J. A., & Taylor, J. H. 1996a, ApJ 469, 819
Camilo, F., Nice, D. J., & Taylor, J. H. 1996b, ApJ 461, 812
Camilo, F., Thorsett, S. E., & Kulkarni, S. R. 1994, ApJ 421, L15
Ghosh, P. & Lamb, F. K. 1979, ApJ 234, 296
Hartman, J.-W., Bhattacharya, D., Wijers, R. A. M. J., & Verbunt, F. 1996, A&A, in press
Kulkarni, S. R. 1986, ApJ 306, L85
Lattimer, J. M. & Yahil, A. 1989, ApJ 340, 420
Meurs, E. J. A. & van den Heuvel, E. P. J. 1989, A&A 226, 88
Romani, R. W. 1990, Nature 347, 741
Romani, R. W. 1993, in Isolated Pulsars. Proceedings of the Los Alamos Workshop held in Taos, New Mexico, February 23–28, 1992, eds. , K. A. Van Riper, R. Epstein, & C. Ho, Los Alamos Natl. Lab. (Cambridge:Cambridge University Press), pp 75–82
Savonije, G. J. 1978, A&A 62, 317
Savonije, G. J. 1979, A&A 71, 352
Seward, F. D. & Mitchell, M. 1981, ApJ 243, 736
Shibazaki, N., Murakami, T., Shaham, J., & Nomoto, K. 1989, Nature 342, 656
Shklovskii, I. S. 1970, Sov. Astron. 13, 562
Srinivasan, G., Bhattacharya, D., Muslimov, A. G., & Tsygan, A. I. 1990, Curr. Sci. 59, 31
Taam, R. E. & van den Heuvel, E. P. J. 1986, ApJ 305, 235
Taylor, J. H., Manchester, R. N., & Lyne, A. G. 1993, ApJS 88, 529
Taylor, J. H., Manchester, R. N., Lyne, A. G., & Camilo, F. 1995, unpublished, available at `ftp://pulsar.princeton.edu/pub/catalog`
Trümper, J., Pietsch, W., Reppin, C., Voges, W., Staubert, R., & Kendziorra, E. 1978, ApJ 221, L105
van den Heuvel, E. P. J. 1994, A&A 291, L39
van den Heuvel, E. P. J. & Bitzaraki, O. 1995, A&A 297, L41
van Kerkwijk, M. H., van Paradijs, J., & Zuiderwijk, E. J. 1995, A&A 303, 497
Verbunt, F., Wijers, R. A. M. J., & Burm, H. M. F. 1990, A&A 234, 195
White, N. E., Swank, J. H., & Holt, S. S. 1983, ApJ 270, 711
Whitlock, L. & Lockner, J. C. 1994, ApJ 437, 841
Wijers, R. A. M. J., Braun, R. I., & Brown, G. E. 1997, in preparation